Properties of low-lying states in ^{65}Co from lifetime measurements

B. Olaizola, L. M. Fraile, H. Mach, F. Nowacki, A. Poves, A. Aprahamian, J. A. Briz, J. Cal-González, D. Ghiţa, U. Köster, W. Kurcewicz, S. R. Lesher, D. Pauwels, E. Picado, D. Radulov, G. S. Simpson, and J. M. Udías

Phys. Rev. C **99**, 024321 — Published 25 February 2019
DOI: 10.1103/PhysRevC.99.024321

Properties of low-lying states in ^{65}Co from lifetime measurements

B. Olaizola,[1,*] L.M. Fraile,[1] H. Mach,[1,2,†] F. Nowacki,[3,4] A. Poves,[5] A. Aprahamian,[6] J.A. Briz,[7,‡] J. Cal-González,[1,§] D. Ghiţa,[8,¶] U. Köster,[9] W. Kurcewicz,[10] S.R. Lesher,[6,11] D. Pauwels,[12] E. Picado,[1,13] D. Radulov,[12,†] G.S. Simpson,[14] and J.M. Udías[1]

[1]*Grupo de Física Nuclear & UPARCOS, Facultad de Físicas, Universidad Complutense - CEI Moncloa, E-28040 Madrid, Spain*
[2]*BP1, NCBJ - National Center for Nuclear Research, Otwock, Poland*
[3]*Université de Strasbourg, IPHC , 23 rue du Loess 67037 Strasbourg, France*
[4]*CNRS, UMR7178, 67037 Strasbourg, France*
[5]*Departamento de Física Teórica and IFT UAM-CSIC, Universidad Autónoma, Cantoblanco, 28049, Madrid, Spain*
[6]*Department of Physics, University of Notre Dame, Notre Dame, Indiana 46556, USA*
[7]*Instituto de Estructura de la Materia, CSIC, E-28006 Madrid, Spain*
[8]*Horia Hulubei National Institute of Physics and Nuclear Engineering, Bucharest, Romania*
[9]*Institut Laue-Langevin, B.P. 156, 38042 Grenoble Cedex 9, France*
[10]*Faculty of Physics, University of Warsaw, Pasteura 5, PL 02-093 Warsaw, Poland*
[11]*Department of Physics, University of Wisconsin - La Crosse, La Crosse, WI 54601, USA*
[12]*K.U. Leuven, IKS, Celestijnenlaan 200 D, 3001 Leuven, Belgium*
[13]*Sección de Radiaciones, Departamento de Física, Universidad Nacional, Heredia, Costa Rica*
[14]*LPSC, Université Grenoble Alpes, CNRS/IN2P3, Institut National Polytechnique de Grenoble, F-38026 Grenoble Cedex, France*

(Dated: February 1, 2019)

The low energy structure of ^{65}Co was studied by means of γ- and fast-timing spectroscopy at the ISOLDE/CERN facility. The known level scheme of ^{65}Co populated following the β^- decay of ^{65}Fe was expanded. The experimental results were compared with large scale shell-model calculations. The measured long lifetime of the $(1/2_1^-)$ level confirms its nature as a highly collective state with proton excitations across the Z=28 gap and neutrons across the N=40 sub-shell.

PACS numbers: 21.10.-k, 21.10.Tg, 23.20.Lv, 27.50.+e,
Keywords: ^{65}Fe, ^{65}Co, ^{65}Ni, β^-, measured γ-γ coincidences, $T_{1/2}$, deduced ^{65}Co B(XL), fast-timing $\beta\gamma\gamma$(t) method, HPGe, $LaBr_3$(Ce) detectors, shell-model calculations

I. INTRODUCTION

The region around ^{68}Ni ($Z = 28$, $N = 40$) has motivated many recent experimental and theoretical studies, aimed at the understanding of the nuclear structure in this region with a large neutron excess. The weakening of the $N = 40$ sub-shell gap just two protons below ^{68}Ni has been documented extensively by deformed ground states in ^{66}Fe [1–4] and ^{64}Cr [5, 6], which was interpreted as the center of the fourth *island of inversion* $N = 40$ by shell-model calculations using the Lenzi-Nowacky-Poves-Sieja (LNPS) interaction [7].

Neutron pair promotions across the $N = 40$ gap are responsible for the deformation of the ground states of the Fe and Cr isotopes and thus have been intensively studied in this region. Due to the persistence of the large energy gap, proton excitations across $Z = 28$ to the *pf* shell are not as well documented. In ^{68}Ni, the 0_3^+ state at 2511 keV (first reported in [8]), has been confirmed to be of proton $2p-2h$ character in a $2p$ transfer reaction [9]. Large scale shell-model calculations required high rank neutron *np-nh* excitations to the $g_{9/2}$ and $d_{5/2}$ orbitals as well as proton excitations across Z=28 to reproduce the energy [7, 10] of this level and B(E2) transition probability to the 2_1^+ state at 2033 keV [11]. In the neighboring ^{66}Ni, this proton-excitation prolate 0^+ was observed at 2965 keV [12]. Shell-model calculations predict that these proton excitations will be more or less constant along the Ni isotopic chain, with such a state as the 0_2^+ at 2.65 MeV in ^{78}Ni [13]. This has been shown as a proof of the persistence of $Z = 28$ shell gap up to $N = 50$.

There is no experimental information on proton excitations available below ^{68}Ni and no such state has been observed in ^{66}Fe as predicted by shell-model calculations at 2.79 MeV [3]. Similar calculations are not yet available for a hypothetical proton excitation state in ^{64}Cr. With an effective single particle energy (ESPE) gap between the $\pi f_{7/2}$ and the *fp* shells of ~ 6 MeV for ^{68}Ni [14, 15], it is not surprising that all proton excitations in the region have been found above 2.5 MeV.

The situation is very different for the odd-A nuclei below Z=28. For the Co chain, only one proton below ^{68}Ni,

* bruno.olaizola@triumf.ca; Present address: TRIUMF, 4004 Wesbrook Mall, Vancouver, British Columbia V6T 2A3, Canada
† Deceased
‡ Present address: CERN, Geneva 23, CH-1211 Switzerland.
§ Present address: Ion Beam Applications, Centro de protón terapia Quirónsalud, Pozuelo de Alarcón, Madrid, Spain
¶ Present address: ELI-NP, 077126 Măgurele, Romania

Pauwels and collaborators [16] were the first to report a $(1/2^-)$ β^--decaying isomer in ^{67}Co (g.s. J^π=$(7/2^-)$) as the first excited state at 491.6 keV. Unlike most other states for odd-A nuclei around ^{68}Ni, this state could not be interpreted as a single particle/hole coupled to the neighboring even-even Ni core. It was, thus, proposed as a proton excitation across the $Z = 28$ gap at an unexpectedly low energy. In a subsequent publication, Pauwels *et al.* [17] identified a similar $(1/2^-)$ state in ^{65}Co that they tentatively proposed as a proton intruder in similarity with ^{67}Co. Unfortunately, realistic shell model interactions for the region were out of reach for the computational power at the time, so calculations were not available to support the proton intruder interpretation of these states. With no additional experimental information, the tentative assignment was only based on systematics.

While in a multinucleon reaction ^{70}Zn+^{238}U Recchia and collaborators [18] did not populate the $(1/2^-)$ states in either ^{65}Co or ^{67}Co, they performed shell-model calculations using the LNPS interaction [7]. Their results clearly showed the presence of a deformed rotational band built on a proton intruder $1/2^-$ in Co isotopes when approaching $N = 40$.

In this paper, we report on the low energy structure of ^{65}Co populated in the β^- decay of ^{65}Mn. Our fast-timing study confirms and expands the level scheme presented in Ref. [17]. More importantly, making use of the advanced time delayed (ATD) method, we measured the lifetimes of the first three excited states (including the $(1/2^-)$ proton intruder state) and set upper limits for another three. We also expand the large scale LNPS calculations presented in Ref. [18], focusing in the ^{65}Co nucleus and on the prolate rotational band.

II. EXPERIMENT

The experiment was performed in the ISOLDE facility at CERN [19]. Isotopes of ^{65}Co were populated in the β^- decay chain of A=65 isobars, starting at ^{65}Mn. The 1.4-GeV protons from the pulsed CERN Proton Synchrotron Booster impinged on an UC_x target in intervals multiple of 1.2 s, inducing high energy fission. The produced radioisotopes were thermally released from the target and manganese atoms were ionized by the ISOLDE Resonance Ionization Laser Ion Source (RILIS) [20]. Ions with A=65 were mass-separated and implanted on a thin aluminum foil in the center of the experimental setup. Without a moving-tape system to remove the decay products, a saturated source was created that included the complete A=65 chain. A fast plastic scintillator acted as β-particle detector and was placed 1-2 mm behind the deposition point. Two truncated-cone shaped $LaBr_3$(Ce) crystals [21] coupled to Photonis XP20D0 photomultipliers were used for γ-ray fast timing. The setup was completed by two HPGe detectors. Analog time-delayed $\beta\gamma(t)$ coincidences between the β and each one of the γ scintillators were set up using constant fraction discriminators (CFD) and time-to-amplitude conversion (TAC) modules. The fast timing analysis is based on $\beta\gamma$ time distributions between the β and $LaBr_3$(Ce) detectors and $\beta\gamma\gamma(t)$ distributions including the former with an additional condition on HPGe energies. Further details on the experimental station and data acquisition strategy can be found in Ref. [22].

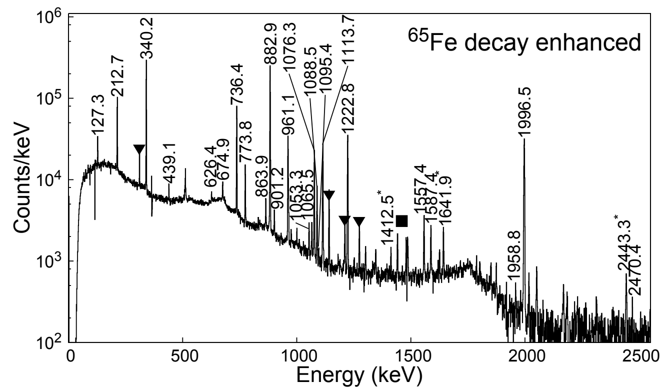

FIG. 1. HPGe energy spectrum with the ^{65}Fe activity enhanced and the ^{65}Co transitions identified; ^{65}Mn activity and long-lived contaminants have been subtracted. *: Transitions observed in the ^{65m}Fe (J^π = $9/2^+$) decay. ▼: transitions observed in ^{65}Ni.

This publication is part of a wider fast timing campaign in which several neutron-rich isotopes below ^{68}Ni were studied [3, 22–25]. A review of the published results so far can be found in [26].

III. EXPERIMENTAL RESULTS

To enhance the ^{65}Fe $\rightarrow$ ^{65}Co decay, a time condition was set between 350 ms and 2399 ms after proton impact on target, when most of the ^{65}Mn had already decayed away. A singles HPGe energy spectrum with this time condition is shown in Fig. 1. The identification of γ rays in ^{65}Co is based on the parent half-life and coincidences with the existing known transitions [17].

Figure 2 shows the $(1/2^-)$ ^{65}Fe ground state half-life measured by gating on the HPGe peaks assigned to ^{65}Co and projected into the time since proton impact. The fit was performed to an exponential decay plus a constant background between the second and third proton in the cycle (between 1.2 and 2.4 seconds after the proton impact on the target). This figure shows the fit of the time distribution gated by the 882.8-keV transition. The final result $T_{1/2}$=805(10) ms is the weighted average of gating different transitions, all in agreement. The contribution from the unobserved background was estimated by adding a constant term to the fit and varying it within a 0 to 50 counts range. The uncertainty has been increased accordingly by 5 ms to account for our

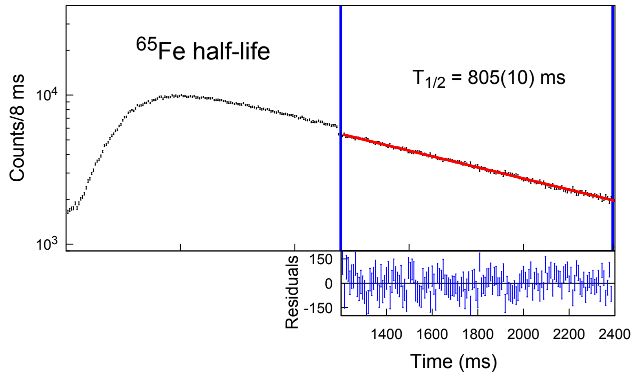

FIG. 2. *(Colour online)* Half-life of the $(1/2^-)$ ^{65}Fe ground state. The exponential fit was done after all the ^{65}Mn had decayed away (between the second and third proton impact of the cycle). See text for details.

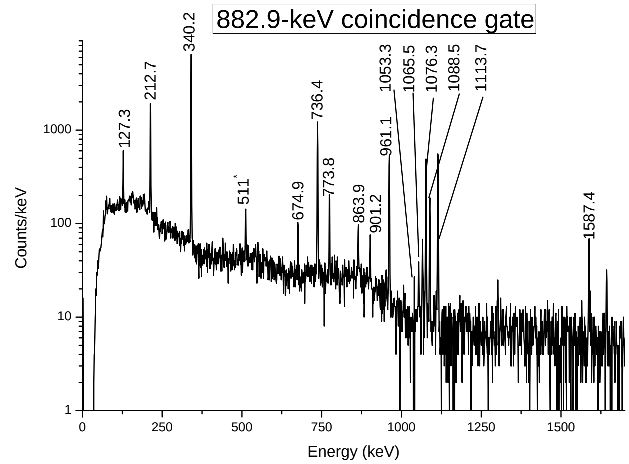

FIG. 3. HPGe-HPGe coincidence energy spectrum with a gate on the 882.8-keV transition in ^{65}Co.

TABLE I. Summary of the observed transitions in the β^- decay of ^{65}Fe to ^{65}Co. Transitions previously observed in the ^{65m}Fe decay have not been included. *: new transitions not observed in [17]. †: intensity obtained from $\gamma\gamma$ coincidences

E_γ (keV)	$E^{\text{level}}_{\text{initial}}$ (keV)	$E^{\text{level}}_{\text{final}}$ (keV)	I^{rel}_γ
127.3(1)	1222.9	1095.6	2.2(2)
212.7(1)	1095.6	882.8	12.5(9)
340.2(1)	1222.9	882.8	51(4)
439.1(1)*	1996.6	1557.5	1.7(1)
626.4(2)*	2184.0	1557.5	0.4(1)
674.9(1)*	1557.5	882.8	1.3(1)
736.4(1)	1959.3	1222.9	26(2)
773.8(1)	1996.6	1222.9	4.6(3)
863.9(1)	1959.3	1095.6	1.4(1)
882.8(1)	882.8	g.s.	100(7)
901.2(1)*	1996.6	1095.6	0.9(1)
961.1(1)†	2184.0	1222.9	14(1)
1053.3(1)*	2276.2	1222.9	0.8(1)
1065.5(1)*	1948.4	882.8	0.9(1)
1076.3(1)	1959.3	882.8	11.1(8)
1088.5(1)	2184.0	1095.6	3.7(3)
1113.7(1)	1996.6	882.8	14(1)
1222.8(1)	1222.9	g.s.	21(2)
1557.4(1)*	1557.5	g.s.	2.3(2)
1587.4(1)*	2470.3	882.8	1.6(1)
1958.8(5)*	1959.3	g.s.	0.1(1)
1996.5(1)	1996.6	g.s.	35(3)
2470.4(5)*	2470.3	g.s.	0.5(1)

TABLE II. Summary of the levels populated in the β decay of ^{65}Fe to ^{65}Co. *: new levels not observed in [17].

E_{level} (keV)	β feeding	log(ft)	$T_{1/2}$ (ps)	J_π
0	-	-		$(7/2^-)$
882.8(1)	5(5)	5.9(5)	4(4)	$(3/2^-)$
1095.6(1)	2.8(6)	6.07(10)	1250(20)	$(1/2^-)$
1222.9(1)	18(3)	5.23(7)	55(6)	$(3/2^-)$
1557.5(1)*	0.9(2)	6.43(10)		
1948.4(1)*	0.6(1)	6.48(8)		
1959.3(1)	24(1)	4.87(4)	< 90	$(1/2, 3/2^-)$
1996.6(1)	35(2)	4.69(2)	< 90	$(3/2^-)$
2184.0(1)	11.2(7)	5.00(2)	< 160	$(1/2, 3/2^-)$
2276.2(1)*	0.5(1)	6.44(9)		
2470.3(2)*	1.3(1)	5.96(4)		

inability to observe and fit this background. The fit was repeated using the Bateman equations fixing the half-life of ^{65}Mn ($T_{1/2}$=91.9(9) ms [23]). The difference was well below the uncertainty (all ^{65}Mn has decayed away at 1.2 s). There are two previous values in the literature; 0.45(15) s [27] and 0.81(5) s [17]. Our result is in agreement with the later and increases its precision.

Table I summarizes the observed γ transitions attributed to ^{65}Co from this work. Pauwels *et al.* [17] proposed two different and independent level schemes for this Co isotope, each one populated by either the $(1/2^-)$ g.s. or the $9/2^+$ β^--decaying isomer of ^{65}Fe. In their work, using a laser ionization, they were able to separate both decays. This is not the case in our work, where we have a cocktail of both decays, so the relative intensities shown correspond to the natural admixture of g.s. and $9/2^+$ isomers populated in the ^{65}Mn β^- decay.

Transitions linking both excited structures have not been observed neither in Ref. [17] nor in our study, so the intensities should be in good agreement between both works. Nevertheless, a number of unobserved high-energy transitions connecting both level schemes cannot be discarded, and this would affect the observed intensity and apparent β feeding.

Figure 4 shows the level scheme of ^{65}Co populated in the β^- decay of the ^{65}Fe $(1/2^-)$ ground state as observed in this work. It was built based in $\gamma\gamma$ coincidences between the two HPGe, as showed in Fig. 3. This level scheme confirms the one reported in Ref. [17] and expands it with 11 new transitions and 4 new levels, due to a factor ~ 1000 increase in HPGe γ-singles statistics.

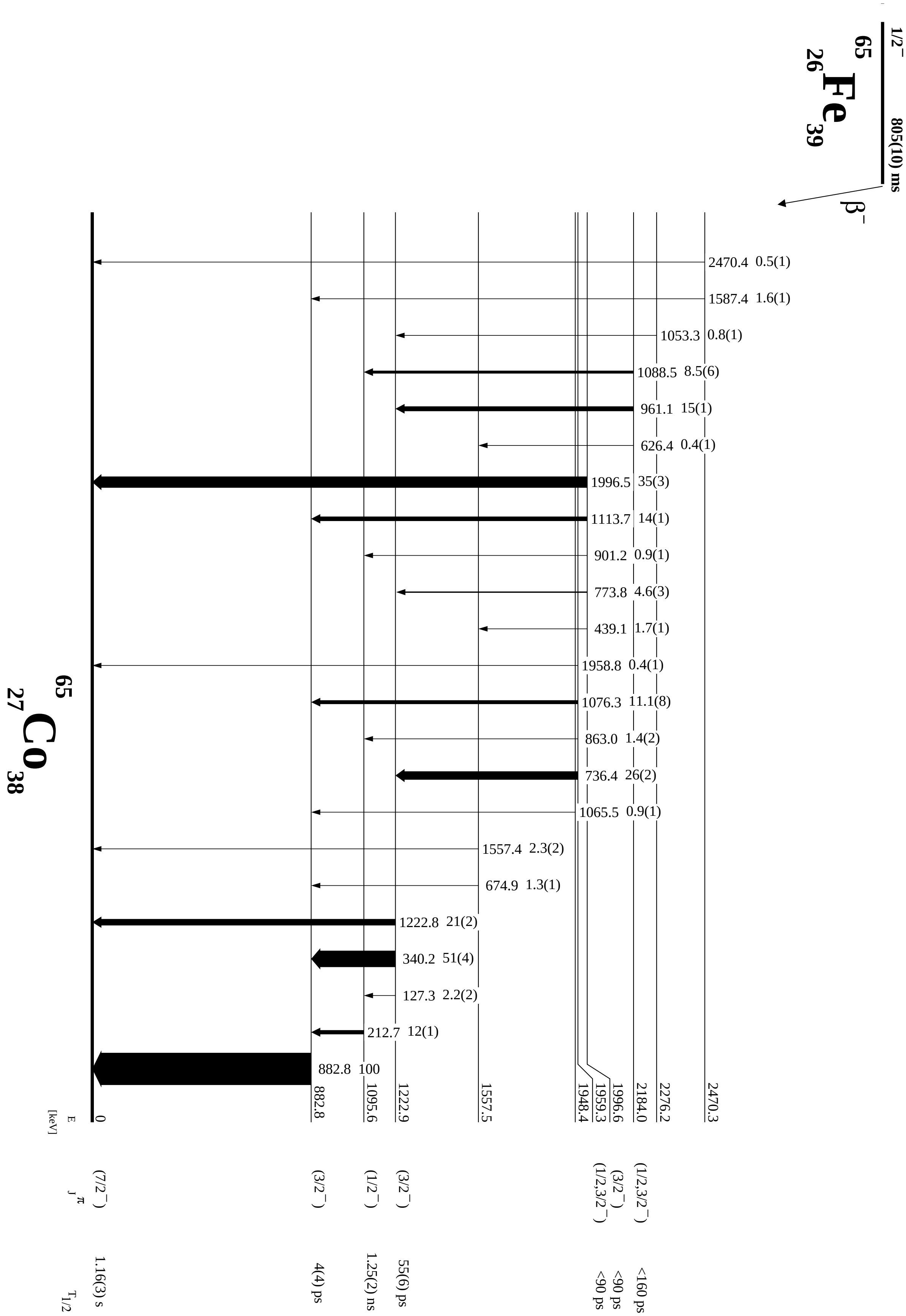

FIG. 4. ^{65}Co level scheme populated in the β decay of ^{65}Fe from this work. Levels and transitions populated in the ^{65m}Fe decay have not been included, even when they were observed in this work.

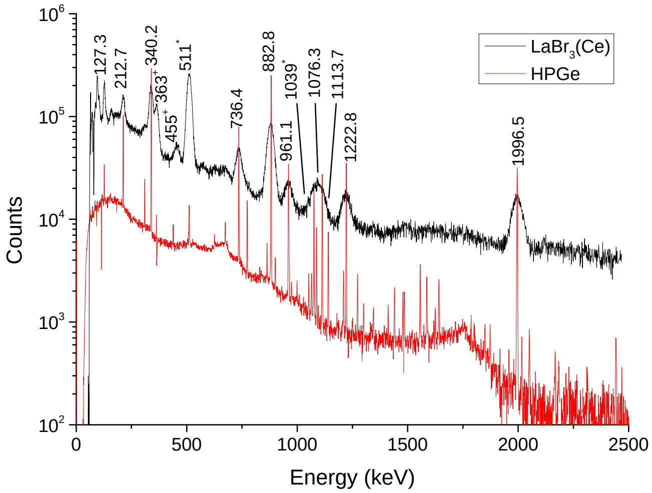

FIG. 5. HPGe (*red*) and $LaBr_3$(Ce) (*black*, renormalized) energy spectra with the ^{65}Fe activity enhanced and the most intense ^{65}Co transitions labeled in keV. It is shown with the same conditions as the fast-timing analysis was performed. $^{+}$: ^{65}Mn decay transitions. *: ^{66}Ga ($T_{1/2}$=9.49(3) h) decay transitions.

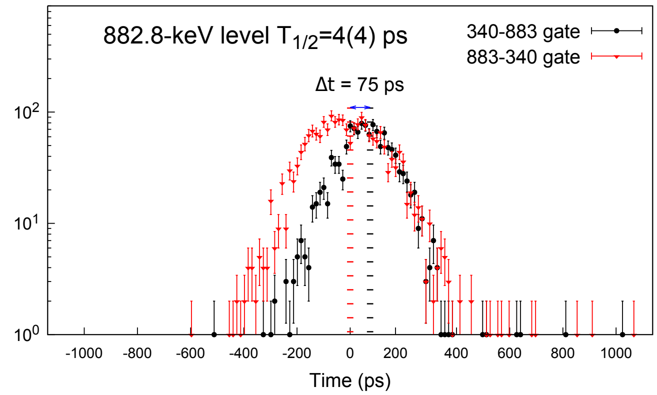

FIG. 6. *(Colour online)* Mean lifetime of the 882.8-keV excited state. *Black circle:* β-340.2(HPGe)-882.8($LaBr_3$(Ce)) coincidence. *Re triangle:* β-882.8(HPGe)-340.2($LaBr_3$(Ce)) coincidence. The $\Delta\tau$ = 75 ps observed must then be corrected by time-walk and the Compton contribution, see text for details

Since the experiment was run with a saturated source, we were able to study the intensity balance of the whole A=65 decay chain. Our results support that there is no direct population of the ground state (upper limit of I_β(g.s) < 0.3%). We have measured this by comparing the intensities in Co and Cu [28]. During this analysis, we were not able to reproduce the intensities of the ^{65}Co $\rightarrow$ ^{65}Ni decay presented in Ref. [17]. The most likely explanation is the very large 92(4)% direct population of the ground state. Any relatively small deviation in that value induces significant changes in the absolute intensity of the observed transitions in ^{65}Ni.

IV. FAST-TIMING ANALYSIS

To extract the excited states lifetimes, we employed the superior timing resolution of the $LaBr_3$(Ce) and plastic scintillator and the ATD $\beta\gamma\gamma$(t) method. Figure 5 shows a $LaBr_3$(Ce) energy spectrum including the time gates used for the fast-timing analysis. The method is thoroughly described in Refs. [29–31] and the particular details for this experiment can be found in [22, 23].

The half-life of the 882.8-keV excited state was measured by the centroid-shift method in $\beta\gamma\gamma$(t) coincidences. Figure 6 shows the time distributions for the β-340.2(HPGe)-882.8($LaBr_3$) and β-882.8(HPGe)-340.2($LaBr_3$) coincidences, with a centroid sift between them of $\Delta\tau$ = 75 ps. To correct the effect of the time walk (despite using CFDs, the detectors present a different time-response for γ-rays of different energies), off-line ^{24}Na, ^{88}Rb and ^{140}Ba sources were employed. These sources have precisely known half-lives in the ps range and cover the energy region of interest. Compton events have a different time response and must be studied independently. Gates were set on the background above the full-energy peaks. Due to the time walk, this Compton time-spectrum was then time-shifted to the right energy using as a reference the Compton background of a ^{24}Na source. See Refs. [22, 23] for additional details on these corrections. The same procedure was repeated with the 1113.7- and 882.8-keV coincidences, measuring independently twice (and each time with two different $LaBr_3$(Ce) crystals). The final result is the weighted average of the four measurements, $T_{1/2}$ = 4(4) ps. The good agreement between the four different measurements and the fact that the final uncertainty is smaller (before rounding) than the value has led us to give a value and not an upper limit.

Using the same technique, but gating on the 340.2- and 736.4-keV transitions, allowed us to obtain a lifetime of $T_{1/2}$ = 55(6) ps for the second ($3/2^-$) state at 1222.9 keV. For the levels at 1959.3, 1996.6 and 2184.0 keV, there was no γ-ray feeding from above, so this method could not be employed. The lack of a delayed component in $\beta\gamma$(t) coincidences, allowed us to set upper limits based on the width of the timing distribution (which strongly depends on the γ-ray energy), see Table II.

The half-life of the 1095.6-keV state was measured in $\beta\gamma$ coincidences de-convoluting the delayed time component from the prompt response by setting a gate on the 212.7-keV transition in the $LaBr_3$(Ce) detectors (see Fig. 7). This result was independently confirmed by gating on the 882.8-keV transition, since the 212.7-keV transition populates the 882.8-keV state, and therefore $\beta\gamma$(t) coincidences will show a contribution from the 1095.6-keV state lifetime. The fit was performed to a Gaussian prompt plus a double exponential decay to account for the Compton background with a shorter lifetime. None

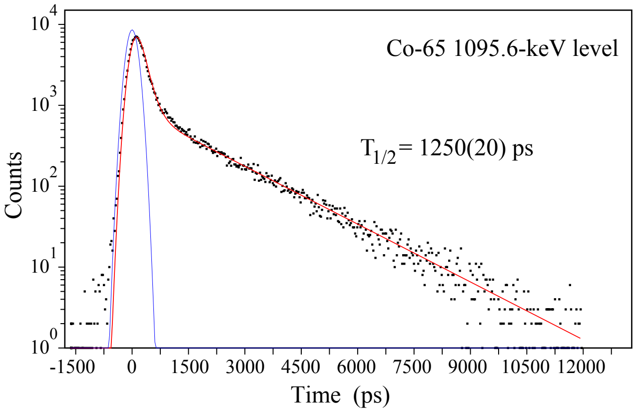

FIG. 7. *(Colour online)* Half-life of the 1095.6-keV state measured in $\beta\gamma$(t) coincidences using the convolution method with a gate on the 212.7-keV transition. The fit was done to a Gaussian prompt plus a double exponential decay.

of the other states with a relatively intense γ ray shows such a long lifetime. Placing a gate in the Compton background next to the 212.7-keV peak did not show a slope either. This unambiguously allowed us to attribute the 1250(20) ps lifetime to the $(1/2^-)$ state at 1095.6 keV. The final result is the weighted average of the four results.

V. SHELL-MODEL CALCULATIONS

To interpret the ^{65}Co experimental results, we performed extensive shell-model calculations using the LNPS effective interaction [7]. In our calculations, ^{48}Ca is taken as a closed core and the valence space includes the complete pf shell for the protons and the $0f_{5/2}$, $1p_{3/2}$, $1p_{1/2}$, $0g_{9/2}$, and $1d_{5/2}$ orbitals for the neutrons. This involves up to 11p-11h excitations across the Z=28 and N=40 gaps. The microscopically derived effective charges of 1.31 for the protons and 0.46 for the neutrons were adopted [33]. The calculations used bare g_l and g_s, since using effective ones gave negligible differences.

The results for the lowest lying states are summarized in Table IV. A very similar structure is found for the $7/2^-$ and $3/2^-$ states and a very distinct one for the $1/2^-$ level. Figure 8 shows a direct comparison of the ground and first $1/2^-$ states. From the calculations results and the long lifetime measured for the 1095.6-keV $(1/2^-)$ state is evident that they are built upon very different configurations. The ground state presents virtually no proton excitations, while for the $1/2^-$ state there is a whole proton excited across the Z=28 gap. Concerning the average neutron orbitals occupation, the ground state has only a single neutron across N=40, which hints to the persistence of said gap in the Co isotopes. For the $1/2^-$ this number goes up to 2.9 and 0.4 towards the $g_{9/2}$ and $d_{5/2}$ orbitals respectively. It is worth mentioning that while the $7/2^-$ and $3/2^-$ states have relatively well

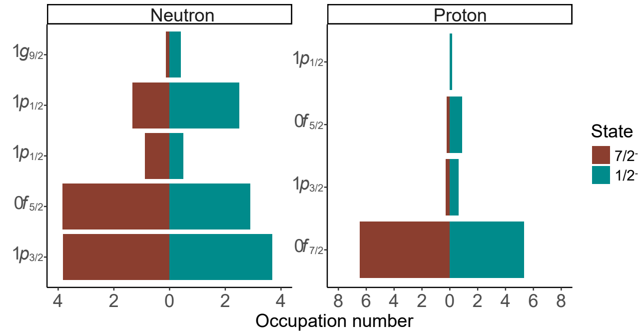

FIG. 8. *(Colour online)* Occupation numbers from the shell model LNPS calculations for neutrons (*left*) and protons (*right*). The blue bars show the occupation of the $7/2^-$ ground state and the red bars of the $1/2^-$ 1095.6-keV state.

defined configurations, with some predominant wavefunctions, the wavefunction of the $1/2^-$ state is completely fragmented, with all configurations having significantly less than a 10% of the weight. This wavefunction fragmentation is characteristic of highly deformed states.

These neutron $2p-2h/4p-4h$ excitations from the pf to the gd orbitals induces the reduction of the $Z = 28$ shell gap by the strong neutron-proton interaction. This favors the proton excitations across Z=28 which, together with the neutrons excited above N=40, produce a deformed solution with K=$1/2^-$. This can be well understood in the Nilsson-SU3 scheme [34], giving rise to an $1/2^-$ state at very low excitation energy with a significant prolate deformation. The calculations predict a $5/2^-$ followed by a $3/2^-$ as continuation of this rotational band, see Fig. 9.

For a more stringent test of the calculations with the shell-model calculations, Table III shows a comparison of measured and calculated transition probabilities. In this table, when both M1 and E2 multipolarities were possible, both are given as pure transitions; i.e. assuming no mixing ratio. There is agreement for the B(E2;$3/2^-_1 \rightarrow 7/2^-_1$) value (the calculated B(E2) yields 8.2 W.u., compared to the 17(16) W.u. measured), although the experimental relative error is nearly 100%. The theoretical calculations uncertainty for small B(M1) is on the order of 10^{-3}, therefore any smaller value has been given as an upper limit. The calculated B(M1;$1/2^-_1 \rightarrow 3/2^-_1$) value is given as an upper limit, but it is also in agreement, within a factor of 2, a reasonable deviation for such a small value. The calculations also predict a negligible mixing ratio δ(E2/M1) for this transition.

Our shell-model calculations also yield four more states below 2 MeV. With the already discussed $3/2^-_1$, they form a quintuplet of states $\{3/2^-, 7/2^-, 11/2^-, 5/2^-, 9/2^-\}$. As discussed in the following section, the combined data from β-decay and reaction experiments allow for the identification of all these states. One additional multiplet of levels is predicted to arise from the coupling $\pi f^{-1}_{7/2} \otimes 3^+$ ^{66}Ni.

TABLE III. Summary of the transition rates obtained in the timing analysis of ^{65}Co and compared to the theoretical calculations. The experimental values for different multipolarities assume pure transitions, they do not arise from measured mixing ratios. See text for details. †: The $(11/2^-)$ 1479.4-keV level is not populated in β decay and was not observed in this experiment. Its lifetime is taken from Ref. [32] and has been included here for comparison with the LNPS calculations.

E_{level} (keV)	J^{π}_i	$T_{1/2}$ (ps)	E_{γ}(keV)	J^{π}_f	Exp. M1(W.u.)	Exp. E2(W.u.)	Calc. M1(W.u.)	Calc. E2(W.u.)
882.8(1)	$(3/2^-_1)$	4(4)	882.8(1)	$(7/2^-_1)$		17(16)		8.2
1095.6(1)	$(1/2^-_1)$	1250(20)	212.7(1)	$(3/2^-_1)$	$1.83(3)\cdot10^{-3}$	67(1)	$<10^{-3}$	0.02
1222.9(1)	$(3/2^-_2)$	55(6)	127.3(1)	$(1/2^-_1)$	$5.8(8)\cdot10^{-3}$	$5.9(8)\cdot10^{2}$	$<10^{-3}$	26.5
			340.2(1)	$(3/2^-_1)$	$7.0(9)\cdot10^{-3}$	100(13)	$<10^{-3}$	0.7
			1222.8(1)	$(7/2^-_1)$	$6.2(9)\cdot10^{-5}$	$6.9(10)\cdot10^{-2}$		
$1479.4(1)^{\dagger}$	$(11/2^-_1)$	0.9(4)	1479.4(1)	$(7/2^-_1)$		5.8(26)		4.1
1959.3(1)	$(1/2, 3/2^-)$	<90	736.4(1)	$(3/2^-_2)$	$>4.1\cdot10^{-4}$	>1.2		
			863.0(1)	$(1/2^-_1)$	$>1.4\cdot10^{-5}$	$>3.0\cdot10^{-2}$		
			1076.3(1)	$(3/2^-_1)$	$>5.6\cdot10^{-5}$	$>8.0\cdot10^{-2}$		
			1958.8(4)	$(7/2^-_1)$		$>1.4\cdot10^{-4}$		
1996.6(1)	$(3/2^-_3)$	<90	439.1(1)		$>8.7\cdot10^{-5}$	$>7.5\cdot10^{-1}$		
			773.8(1)	$(3/2^-_2)$	$>4.3\cdot10^{-5}$	$>1.9\cdot10^{-1}$		
			901.2(1)	$(1/2^-_1)$	$>5.6\cdot10^{-6}$	$>1.1\cdot10^{-2}$		
			1113.7(1)	$(3/2^-_1)$	$>4.4\cdot10^{-5}$	$>5.9\cdot10^{-2}$		
			1996.5(1)	$(7/2^-_1)$		$>7.9\cdot10^{-3}$		
2184.0(1)	$(1/2, 3/2^-)$	<180	626.4(1)		$>8.3\cdot10^{-6}$	$>3.5\cdot10^{-2}$		
			961.1(1)	$(3/2^-_2)$	$>8.6\cdot10^{-5}$	$>1.5\cdot10^{-1}$		
			1088.5(1)	$(1/2^-_1)$	$>3.4\cdot10^{-5}$	$>4.7\cdot10^{-2}$		

TABLE IV. Calculated ^{65}Co level scheme in the valence space $\nu(1p_{3/2}\ 0f_{5/2},\ 1p_{1/2},\ 0g_{9/2},\ 1d_{5/2})$ and $\pi(0f_{7/2},\ 1p_{3/2},\ 0f_{5/2},\ 1p_{1/2})$. The proton and neutron occupation columns list the average occupations of the valence orbitals.

		Proton occupation numbers				Neutron occupation numbers				
Elevel (keV)	J^{π}	$0f_{7/2}$	$1p_{3/2}$	$0f_{5/2}$	$1p_{1/2}$	$1p_{3/2}$	$0f_{5/2}$	$1p_{1/2}$	$1g_{9/2}$	$1d_{5/2}$
0	$7/2^-$	6.48	0.29	0.21	0.02	3.82	3.84	0.88	1.33	0.13
1070	$3/2^-$	6.28	0.45	0.25	0.03	3.83	3.93	0.96	1.20	0.08
1290	$1/2^-$	5.31	0.63	0.89	0.17	3.68	2.90	0.50	2.51	0.41

We obtained a third $3/2^-$ state with this configuration at 1.84 MeV, with an additional $1/2^-$ spherical state in the same energy range. The experimentally observed states at 1959.3, 1996.6 and 2184.0 keV (tentatively $1/2, 3/2^-$), are natural candidates, see Fig. 9.

VI. DISCUSSION

During this study we found no evidence to contradict the spin-parity assignments suggested for ^{65}Co in Ref. [17] therefore, while tentative, they will be accepted for the following discussion.

The $(7/2^-)$ ground state can be interpreted as the coupling of a $\pi f^{-1}_{7/2}$ to either the ground state of ^{66}Ni or ^{64}Fe. The ground state of ^{64}Fe has been demonstrated to be deformed [2, 35, 36], while for ^{66}Ni it is expected to be spherical or slightly oblate [12, 25]. The proton and neutron occupancies from our shell-model calculations show very little to no deformation for the ^{65}Co ground state, favouring the interpretation of the coupling to the Ni core.

Likewise, Modamio *el al.* [32] confirmed through lifetime measurements the $\pi f^{-1}_{7/2} \otimes ^{66}\text{Ni}(2^+_1)$ character of the $(9/2^-)$ and $(11/2^-)$ states. The tentative $(5/2^-, 7/2^-)$ states observed by Pauwels *et al.* [17] at 1441.1 and 1625.5 keV are candidates to belong to this $\pi f^{-1}_{7/2} \otimes {}^{\text{A+1}}\text{Ni}(2^+_1)$ quintuplet. The ordering in our shell-model calculations favours the assignment of the 1441.1-keV state as $7/2^-$ and the 1625.5 keV one as $5/2^-$, see Fig. 9.

Due to the large energy difference between the $(3/2^-_1)$ state and the observed $(9/2^-_1)$, a later interpretation ruled out the $(3/2^-_1)$ states as part of that quintuplet [18]. However, the shell-model calculations presented in this work, using a much larger model space, correctly predict the energy of this $(3/2^-_1)$ state and assign it as part of the quintuplet. Moreover, the calculated spherical shape of the state also hints at the coupling to the more spherical Ni isotopes. It seems a well established interpretation of the ground state and the quintuplet $\{3/2^-, 5/2^-, 7/2^-, 9/2^-, 11/2^-\}$ as a proton $\pi f^{-1}_{7/2}$ hole coupled to ^{66}Ni 2^+_1 state.

Originally, it was suggested that the $3/2^-_1$ states in the Co isotopes were built on the coupling $\pi f^{-1}_{7/2} \otimes {}^{\text{A-1}}\text{Fe}(2^+_1)$

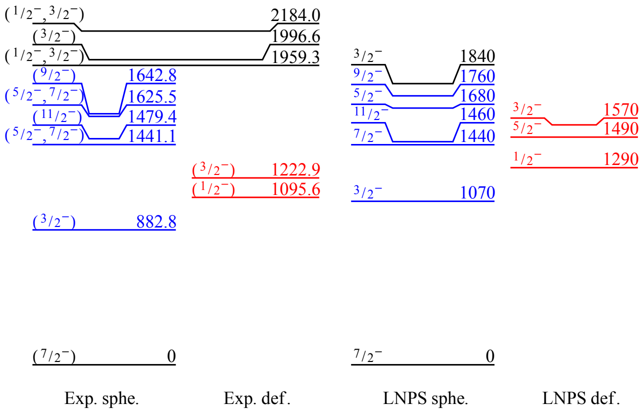

FIG. 9. *(Colour online)* Comparison of experimental (*left*) and calculated (*right*) level schemes. The levels in blue correspond to the spherical $\pi f_{7/2}^{-1} \otimes^{66}\mathrm{Ni}(2_1^+)$ quintuplet, while the levels in red are the deformed K=1/2 band. The experimental levels not observed in this work are extracted from [18].

based on the Co and Fe energy systematics [16, 17]. Subsequent studies discarded this interpretation claiming a lack of correlation between the B(E2) strengths of the levels [18, 32, 37]. As shown above, the B(E2;$3/2_1^- \rightarrow 7/2_1^-$) in ^{A}Co should instead be compared with the B(E2;$2_1^+ \rightarrow 0_1^+$) in $^{A+1}$Ni. In the lighter isotopes (N=30-34(36)), the B(E2) values follow a parallel trend for Fe, Co and Ni, although the Co values are somehow closer to those in Ni. For N=38 (and to a lesser extent N=36) the B(E2) systematics of Fe and Ni diverge. Fe already belongs to the N=40 island of inversion and its collectivity is rapidly increasing with larger B(E2) values, while for Ni the B(E2) rates are decreasing as they approach the N=40 local shell closure. The large uncertainty in the measured ^{65}Co B(E2)=17(16) W.u. does not allow for reliable comparisons, but the theoretical 8.2 W.u. may shed some light into the matter. This calculated value compares better with the 7.6(13) W.u. value in ^{66}Ni rather than with the much larger 22.7(2) W.u. in ^{64}Fe [38]. It seems, then, that the B(E2) systematics also support the interpretation of the $3/2_1^-$ states belonging to the $\pi f_{7/2}^{-1} \otimes \mathrm{Ni}(2_1^+)$ quintuplet.

It is tempting to interpret the 1095-keV $1/2_1^-$ state as a single proton promoted to the $1p_{1/2}$ orbital coupled to the 0^+ state in ^{66}Ni, but as we can see in Fig. 8, the situation is far more complex. While there is indeed the promotion of one proton from the $0f_{7/2}$ orbital to the pf one, we can see how the wave function is completely fragmented, the occupation number of this excited proton is distributed along the three suborbitals $1p_{3/2}$, $0f_{5/2}$ and $1p_{1/2}$. In this naive interpretation of a single proton excitation, we would expect the neutrons to remain paired and not contributing to the total J$^\pi$ of the state. But once again the nature of the level is more intricate, involving several neutron excitations up to the $1d_{5/2}$ orbital, with many possible wavefunctions including unpaired nucleons. This is characteristic of highly deformed shapes, where a large number of particles are involved in highly collective states.

The ($3/2_2^-$) state was interpreted in Ref. [18] as part of the quintuplet of the coupling of the proton hole to the ^{66}Ni 2_1^+ state, but, as discussed previously, we favour the assignment of the ($3/2_1^-$) state for this quintuplet. The other possible origin of the state is that it belongs to the rotational band built on the ($1/2_1^-$) proton intruder. The B(M1) are evenly split towards the ($1/2_1^-$) and the ($3/2_1^-$), with only the transition to the ($7/2^-$) g.s. suppressed. This makes for a difficult interpretation. The possibility of the ($3/2_2^-$) being instead a ($5/2_1^-$) can be discarded by the presence of the 127.3-keV transition to the prolate ($1/2_1^-$) state. With the lifetime measured in this work, it would yield an unrealistic B(E2)=590(80) W.u. (see Table III).

In the shell-model calculations, the deformed $5/2_1^-$ obtained appears below the $3/2^-$ of the K=1/2 band. So far, no experiment has observed a candidate for such state. The small energy gap between the detected $1/2_1^-$ and $3/2_2^-$ (only 127.3 keV), suggests that any hypothetical intraband transition connecting the $5/2_1^-$ level would have very low energy. Observation of a weak 60-70 keV transition is complicated by the strong presence of x-rays and the low efficiency of our HPGe detectors for that energy range. The calculations also predict that the interband transitions are strongly suppressed, which could explain why this experiment has not observed transitions decaying from a possible $5/2^-$ level to the lower spherical $3/2^-$ or $7/2^-$.

VII. CONCLUSIONS

In this work we have measured the lifetime of the first three excited states in ^{65}Co, providing the first empirical proof of shape coexistence in the nucleus. The $7/2^-$ g.s. and the $3/2_1^-$ $9/2_1^-$, $11/2_1^-$ and the two tentative $(5/2, 7/2)^-$ levels can be interpreted as spherical states of a proton hole in the $\pi 0f_{7/2}$ orbital coupled to the spherical ground and 2_1^+ states in ^{66}Ni. Simultaneously a set of deformed, highly-collective states ($1/2_1^-$ and $3/2_2^-$) are built on high-rank $np - nh$ configurations. LNPS calculations have shown that these are complex states with very fragmented wavefunction that requires several excitations across the Z=28 and N=40,50 gaps.

ACKNOWLEDGMENTS

This work was partially supported by the Spanish MINECO through projects FPA2014-57196, FPA2015-65035-P and Centro de Excelencia Severo Ochoa Programme (SEV-2016-0597). Support by Grupo de Física Nuclear (GFN-UCM) and by the European Union Seventh Framework through ENSAR (contract no. 262010) is also acknowledged. B.O. acknowledges funding by the CPAN project. S.R.L. acknowledge funding by the US National Science Foundation under contract PHY-07-58100. The authors thank Dr. L. Toker for her invaluable help preparing the figures for this manuscript.

[1] M. Hannawald, T. Kautzsch, A. Wöhr, W. B. Walters, K.-L. Kratz, V. N. Fedoseyev, V. I. Mishin, W. Böhmer, B. Pfeiffer, V. Sebastian, Y. Jading, U. Köster, J. Lettry, H. L. Ravn, and the ISOLDE Collaboration, Phys. Rev. Lett. **82**, 1391 (1999).

[2] W. Rother, A. Dewald, H. Iwasaki, S. M. Lenzi, K. Starosta, D. Bazin, T. Baugher, B. A. Brown, H. L. Crawford, C. Fransen, A. Gade, T. N. Ginter, T. Glasmacher, G. F. Grinyer, M. Hackstein, G. Ilie, J. Jolie, S. McDaniel, D. Miller, P. Petkov, T. Pissulla, A. Ratkiewicz, C. A. Ur, P. Voss, K. A. Walsh, D. Weisshaar, and K.-O. Zell, Phys. Rev. Lett. **106**, 022502 (2011).

[3] B. Olaizola, L. M. Fraile, H. Mach, A. Poves, A. Aprahamian, J. A. Briz, J. Cal-Gonzlez, D. Ghia, U. Kster, W. Kurcewicz, S. R. Lesher, D. Pauwels, E. Picado, D. Radulov, G. S. Simpson, and J. M. Udas, Journal of Physics G: Nuclear and Particle Physics **44**, 125103 (2017).

[4] M. Stryjczyk, Y. Tsunoda, I. G. Darby, H. De Witte, J. Diriken, D. V. Fedorov, V. N. Fedosseev, L. M. Fraile, M. Huyse, U. Köster, B. A. Marsh, T. Otsuka, D. Pauwels, L. Popescu, D. Radulov, M. D. Seliverstov, A. M. Sjödin, P. Van den Bergh, P. Van Duppen, M. Venhart, W. B. Walters, and K. Wimmer, Phys. Rev. C **98**, 064326 (2018).

[5] A. Gade, R. V. F. Janssens, T. Baugher, D. Bazin, B. A. Brown, M. P. Carpenter, C. J. Chiara, A. N. Deacon, S. J. Freeman, G. F. Grinyer, C. R. Hoffman, B. P. Kay, F. G. Kondev, T. Lauritsen, S. McDaniel, K. Meierbachtol, A. Ratkiewicz, S. R. Stroberg, K. A. Walsh, D. Weisshaar, R. Winkler, and S. Zhu, Phys. Rev. C **81**, 051304(R) (2010).

[6] H. L. Crawford, R. M. Clark, P. Fallon, A. O. Macchiavelli, T. Baugher, D. Bazin, C. W. Beausang, J. S. Berryman, D. L. Bleuel, C. M. Campbell, M. Cromaz, G. de Angelis, A. Gade, R. O. Hughes, I. Y. Lee, S. M. Lenzi, F. Nowacki, S. Paschalis, M. Petri, A. Poves, A. Ratkiewicz, T. J. Ross, E. Sahin, D. Weisshaar, K. Wimmer, and R. Winkler, Phys. Rev. Lett. **110**, 242701 (2013).

[7] S. M. Lenzi, F. Nowacki, A. Poves, and K. Sieja, Phys. Rev. C **82**, 054301 (2010).

[8] W. F. Mueller, B. Bruyneel, S. Franchoo, M. Huyse, J. Kurpeta, K. Kruglov, Y. Kudryavtsev, N. V. S. V. Prasad, R. Raabe, I. Reusen, P. Van Duppen, J. Van Roosbroeck, L. Vermeeren, L. Weissman, Z. Janas, M. Karny, T. Kszczot, A. Płochocki, K.-L. Kratz, B. Pfeiffer, H. Grawe, U. Köster, P. Thirolf, and W. B. Walters, Phys. Rev. C **61**, 054308 (2000).

[9] C. J. Chiara, R. Broda, W. B. Walters, R. V. F. Janssens, M. Albers, M. Alcorta, P. F. Bertone, M. P. Carpenter, C. R. Hoffman, T. Lauritsen, A. M. Rogers, D. Seweryniak, S. Zhu, F. G. Kondev, B. Fornal, W. Królas, J. Wrzesiński, N. Larson, S. N. Liddick, C. Prokop, S. Suchyta, H. M. David, and D. T. Doherty, Phys. Rev. C **86**, 041304 (2012).

[10] Y. Tsunoda, T. Otsuka, N. Shimizu, M. Honma, and Y. Utsuno, Phys. Rev. C **89**, 031301 (2014).

[11] B. Crider, C. Prokop, S. Liddick, M. Al-Shudifat, A. Ayangeakaa, M. Carpenter, J. Carroll, J. Chen, C. Chiara, H. David, A. Dombos, S. Go, R. Grzywacz, J. Harker, R. Janssens, N. Larson, T. Lauritsen, R. Lewis, S. Quinn, F. Recchia, A. Spyrou, S. Suchyta, W. Walters, and S. Zhu, Physics Letters B **763**, 108 (2016).

[12] S. Leoni, B. Fornal, N. Mărginean, M. Sferrazza, Y. Tsunoda, T. Otsuka, G. Bocchi, F. C. L. Crespi, A. Bracco, S. Aydin, M. Boromiza, D. Bucurescu, N. Cieplicka-Oryǹczak, C. Costache, S. Călinescu, N. Florea, D. G. Ghiţă, T. Glodariu, A. Ionescu, L. Iskra, M. Krzysiek, R. Mărginean, C. Mihai, R. E. Mihai, A. Mitu, A. Negreţ, C. R. Niţă, A. Olăcel, A. Oprea, S. Pascu, P. Petkov, C. Petrone, G. Porzio, A. Şerban, C. Sotty, L. Stan, I. Ştiru, L. Stroe, R. Şuvăilă, S. Toma, A. Turturică, S. Ujeniuc, and C. A. Ur, Phys. Rev. Lett. **118**, 162502 (2017).

[13] F. Nowacki, A. Poves, E. Caurier, and B. Bounthong, Phys. Rev. Lett. **117**, 272501 (2016).

[14] T. Otsuka, T. Suzuki, R. Fujimoto, H. Grawe, and Y. Akaishi, Phys. Rev. Lett. **95**, 232502 (2005).

[15] T. Otsuka, T. Suzuki, M. Honma, Y. Utsuno, N. Tsunoda, K. Tsukiyama, and M. Hjorth-Jensen, Phys. Rev. Lett. **104**, 012501 (2010).

[16] D. Pauwels, O. Ivanov, N. Bree, J. Büscher, T. E. Cocolios, J. Gentens, M. Huyse, A. Korgul, Y. Kudryavtsev, R. Raabe, M. Sawicka, I. Stefanescu, J. Van de Walle, P. Van den Bergh, P. Van Duppen, and W. B. Walters, Phys. Rev. C **78**, 041307 (2008).

[17] D. Pauwels, O. Ivanov, N. Bree, J. Büscher, T. E. Cocolios, M. Huyse, Y. Kudryavtsev, R. Raabe, M. Sawicka, J. V. de Walle, P. V. Duppen, A. Korgul, I. Stefanescu, A. A. Hecht, N. Hoteling, A. Wöhr, W. B. Walters, R. Broda, B. Fornal, W. Krolas, T. Pawlat, J. Wrzesinski, M. P. Carpenter, R. V. F. Janssens, T. Lauritsen, D. Seweryniak, S. Zhu, J. R. Stone, and X. Wang, Phys. Rev. C **79**, 044309 (2009).

[18] F. Recchia, C. J. Chiara, R. V. F. Janssens, D. Weisshaar, A. Gade, W. B. Walters, M. Albers, M. Alcorta, V. M. Bader, T. Baugher, D. Bazin, J. S. Berryman, P. F. Bertone, B. A. Brown, C. M. Campbell, M. P. Carpenter, J. Chen, H. L. Crawford, H. M. David, D. T. Doherty, C. R. Hoffman, F. G. Kondev, A. Korichi, C. Langer, N. Larson, T. Lauritsen, S. N. Liddick, E. Lunderberg, A. O. Macchiavelli, S. Noji, C. Prokop, A. M. Rogers, D. Seweryniak, S. R. Stroberg, S. Suchyta, S. Williams, K. Wimmer, and S. Zhu, Phys. Rev. C **88**, 041302 (2013).

[19] E. Kugler, Hyperfine Interactions **129**, 23 (2000).

[20] V. Fedoseyev, K. Batzner, R. Catherall, A. Evensen, D. Forkel-Wirth, O. Jonsson, E. Kugler, J. Lettry, V. Mishin, H. Ravn, and G. Weyer, Nuclear Instruments and Methods in Physics Research Section B: Beam Interactions with Materials and Atoms **126**, 88 (1997), inter-

national Conference on Electromagnetic Isotope Separators and Techniques Related to Their Applications.

[21] V. Vedia, M. Carmona-Gallardo, L. M. Fraile, H. Mach, and J. M. Udías, Nuclear Instruments and Methods in Physics Research Section A: Accelerators, Spectrometers, Detectors and Associated Equipment **857**, 98 (2017).

[22] B. Olaizola, *Ultra-fast timing study of exotic neutron-rich isotopes*, Ph.D. thesis, Universidad Complutense de Madrid, España (2013).

[23] B. Olaizola, L. M. Fraile, H. Mach, A. Aprahamian, J. A. Briz, J. Cal-González, D. Ghiţa, U. Köster, W. Kurcewicz, S. R. Lesher, D. Pauwels, E. Picado, A. Poves, D. Radulov, G. S. Simpson, and J. M. Udías, Phys. Rev. C **88**, 044306 (2013).

[24] B. Olaizola, L. M. Fraile, H. Mach, A. Aprahamian, J. A. Briz, J. Cal-González, D. Ghiţa, U. Köster, W. Kurcewicz, S. R. Lesher, D. Pauwels, E. Picado, A. Poves, D. Radulov, G. S. Simpson, and J. M. Udías, JPS Conf. Proc **6**, 030006 (2015).

[25] B. Olaizola, L. M. Fraile, H. Mach, A. Poves, F. Nowacki, A. Aprahamian, J. A. Briz, J. Cal-González, D. Ghiţa, U. Köster, W. Kurcewicz, S. R. Lesher, D. Pauwels, E. Picado, D. Radulov, G. S. Simpson, and J. M. Udías, Phys. Rev. C **95**, 061303 (2017).

[26] L. M. Fraile, Journal of Physics G: Nuclear and Particle Physics **44**, 094004 (2017).

[27] S. Czajkowski, M. Bernas, P. Armbruster, H. Geissel, C. Kozhuharov, G. Munzenberg, D. Vieira, P. Dessagne, C. Miehe, E. Hanelt, G. Audi, and J. K. P. Lee, Z. Phys. **A348**, 267 (1994).

[28] E. Browne and J. Tuli, Nuclear Data Sheets **111**, 2425 (2010).

[29] H. Mach, R. Gill, and M. Moszyński, Nuclear Instruments and Methods in Physics Research Section A: Accelerators, Spectrometers, Detectors and Associated Equipment **280**, 49 (1989).

[30] M. Moszyński and H. Mach, Nuclear Instruments and Methods in Physics Research Section A: Accelerators, Spectrometers, Detectors and Associated Equipment **277**, 407 (1989).

[31] H. Mach, F. Wohn, G. Molnár, K. Sistemich, J. C. Hill, M. Moszyński, R. Gill, W. Krips, and D. Brenner, Nuclear Physics A **523**, 197 (1991).

[32] V. Modamio, J. J. Valiente-Dobón, S. Lunardi, S. M. Lenzi, A. Gadea, D. Mengoni, D. Bazzacco, A. Algora, P. Bednarczyk, G. Benzoni, B. Birkenbach, A. Bracco, B. Bruyneel, A. Bürger, J. Chavas, L. Corradi, F. C. L. Crespi, G. de Angelis, P. Désesquelles, G. de France, R. Depalo, A. Dewald, M. Doncel, M. N. Erduran, E. Farnea, E. Fioretto, C. Fransen, K. Geibel, A. Gottardo, A. Görgen, T. Habermann, M. Hackstein, H. Hess, T. Hüyük, P. R. John, J. Jolie, D. Judson, A. Jungclaus, N. Karkour, R. Kempley, S. Leoni, B. Melon, R. Menegazzo, C. Michelagnoli, T. Mijatović, B. Million, O. Möller, G. Montagnoli, D. Montanari, A. Nannini, D. R. Napoli, Z. Podolyak, G. Pollarolo, A. Pullia, B. Quintana, F. Recchia, P. Reiter, D. Rosso, W. Rother, E. Sahin, M. D. Salsac, F. Scarlassara, K. Sieja, P. A. Söderström, A. M. Stefanini, O. Stezowski, S. Szilner, C. Theisen, B. Travers, and C. A. Ur, Phys. Rev. C **88**, 044326 (2013).

[33] M. Dufour and A. P. Zuker, Phys. Rev. C **54**, 1641 (1996).

[34] A. P. Zuker, A. Poves, F. Nowacki, and S. M. Lenzi, Phys. Rev. C **92**, 024320 (2015).

[35] J. Ljungvall, A. Görgen, A. Obertelli, W. Korten, E. Clément, G. de France, A. Bürger, J.-P. Delaroche, A. Dewald, A. Gadea, L. Gaudefroy, M. Girod, M. Hackstein, J. Libert, D. Mengoni, F. Nowacki, T. Pissulla, A. Poves, F. Recchia, M. Rejmund, W. Rother, E. Sahin, C. Schmitt, A. Shrivastava, K. Sieja, J. J. Valiente-Dobón, K. O. Zell, and M. Zielińska, Phys. Rev. C **81**, 061301 (2010).

[36] M. Klintefjord, J. Ljungvall, A. Görgen, S. M. Lenzi, F. L. Bello Garrote, A. Blazhev, E. Clément, G. de France, J.-P. Delaroche, P. Désesquelles, A. Dewald, D. T. Doherty, C. Fransen, A. Gengelbach, G. Georgiev, M. Girod, A. Goasduff, A. Gottardo, K. Hadyńska-Klęk, B. Jacquot, T. Konstantinopoulos, A. Korichi, A. Lemasson, J. Libert, A. Lopez-Martens, C. Michelagnoli, A. Navin, J. Nyberg, R. M. Pérez-Vidal, S. Roccia, E. Sahin, I. Stefan, A. E. Stuchbery, M. Zielińska, D. Barrientos, B. Birkenbach, A. Boston, L. Charles, M. Ciemala, J. Dudouet, J. Eberth, A. Gadea, V. González, L. Harkness-Brennan, H. Hess, A. Jungclaus, W. Korten, R. Menegazzo, D. Mengoni, B. Million, A. Pullia, D. Ralet, F. Recchia, P. Reiter, M. D. Salsac, E. Sanchis, O. Stezowski, C. Theisen, and J. J. Valiente Dobon, Phys. Rev. C **95**, 024312 (2017).

[37] A. Dijon, E. Clément, G. de France, P. Van Isacker, J. Ljungvall, A. Görgen, A. Obertelli, W. Korten, A. Dewald, A. Gadea, L. Gaudefroy, M. Hackstein, D. Mengoni, T. Pissulla, F. Recchia, M. Rejmund, W. Rother, E. Sahin, C. Schmitt, A. Shrivastava, J. J. Valiente-Dobón, K. O. Zell, and M. Zieliska, Phys. Rev. C **83** (2011), 10.1103/PhysRevC.83.064321.

[38] B. Pritychenko, M. Birch, B. Singh, and M. Horoi, Atomic Data and Nuclear Data Tables **107**, 1 (2016).